Phonon and Raman spectra: effect of interface diffusion of strained Si/Ge superlattices

1991 J. Phys.: Condens. Matter 3 6239

(http://iopscience.iop.org/0953-8984/3/33/003)

J. Phys.: Condens. Matter 3 (1991) 6239–6248. Printed in the UK

Phonon and Raman spectra: effect of interface diffusion of strained Si/Ge superlattices

Jian Zi, Kaiming Zhang and Xide Xie
CCAST (World Laboratory), PO Box 8730, Beijing 100080 and Department of Physics, Fudan University, Shanghai 200433, People's Republic of China

Received 6 December 1990

Abstract. Phonon and Raman spectra of strained $(Si)_n(Ge)_m$ $(n + m = 8, 2 \leq n \leq 6)$ superlattices grown pseudomorphically on a (001)-oriented Si substrate are studied theoretically using a generalized two-parameter Keating model. It is found that the phonon frequencies of Si-like confined longitudinal (LO) modes are well described by the bulk dispersion curves with the effective number of Si layers given by $n_{\text{eff}} = n + 1$, whereas for Ge-like longitudinal confined modes the confinement is quite complex because of overlapping of the optical continuum of Ge with the acoustical continuum of Si. Phonon frequency shifts of confined modes due to interface diffusion are discussed within the virtual-crystal approximation.

1. Introduction

Owing to its excellent etching and mechanical properties, silicon has been an indispensable material in microelectronic technology. Being an indirect-gap semiconductor, silicon has been excluded from many applications, such as devices in photonics and optoelectronics. The improvement of the electronic properties of this material has aroused the continuing interest of scientists. With the rapid progress of some new growth techniques, such as molecular beam epitaxy (MBE), ultrathin Si/Ge superlattices have been successfully produced [1] in spite of the large lattice mismatch (4.2%) between Si and Ge.

Most of the experimental information on superlattice phonons is obtained by Raman spectroscopy, which probes phonons with wavevectors near the zone centre [1]. Several theoretical models have been adopted to study the phonon spectra of strained Si/Ge superlattices. Using a linear-chain model and neglecting the strain, phonon spectra of Si/Ge superlattices have recently been calculated by Fasolino *et al* [2]. Many interesting features of the phonon modes in the Si/Ge system have been found and discussed. Phonon spectra of several Si/Ge superlattices with different space groups have been investigated by Alonso *et al* [3] on the basis of three-dimensional formalism developed by Kanellis [4] and the two-parameter Keating model [5], neglecting the effect of strain. Incorporating strain, Ghanbari and Fasol [6] studied the phonons of Si/Ge superlattices with a modified six-parameter valence force potential model. More recently, using a generalized Keating model and taking strain into account, Zi *et al* [7, 8] discussed phonons, geometrical structures and growth.

0953-8984/91/336239 + 10 $03.50

As a consequence of the superperiodicity in superlattices, in addition to the reduction in the symmetry, some novel features also appear. The phonon spectra in superlattices are sensitive to many structural properties such as the composition, the overall period and the individual layer thickness and also to the quality and composition of the interface. The large superlattice period leads to many modes in the reduced superlattice Brillouin zone. The phonon modes in superlattices are generally divided into four types: confined modes, resonant quasi-confined modes, interface modes and folded modes. Folding and confinement in the phonon modes of superlattices are usually understood by means of matching of the bulk solutions at the interface [9]. When a mode falls into a gap of the bulk continuum of either constituent, vibrations of sublattice atoms are forbidden; hence this mode can only be strongly localized at interfaces and its vibrations decay exponentially. These modes are interface modes. In the case of Si/Ge superlattices, the longitudinal phonon continuum of bulk Ge fully overlaps with that of Si. Therefore, some modes with strong resonance, the so-called resonant quasi-confined modes, can exist just below the edge of overlapping frequencies with behaviour similar to that of the true confined modes [10]. Hence the Ge-like longitudinal optical (LO) mode can only be the resonant quasi-confined mode.

In the present work the phonon and Raman spectra of strained $(Si)_n/(Ge)_m$ $(n + m = 8, 2 \leqslant n \leqslant 6)$ superlattices grown pseudomorphically on a (001)-oriented Si substrate are investigated. Within the virtual-crystal approximation, the effect of interface diffusion on phonon frequencies is evaluated.

2. Phonon spectra of $(Si)_n/(Ge)_m$

Most Raman scattering experiments have been done in the back-scattering configuration which allows only the longitudinal phonons propagating in the [001] direction from the selection rules. Therefore our discussion is restricted here to the longitudinal phonons in the [001] direction for $(Si)_n/(Ge)_m$ $(n + m = 8, 2 \leqslant n \leqslant 6)$ superlattices grown pseudomorphically on a Si(001) substrate.

A generalized two-parameter Keating model [7, 8], which involves bond-stretching (α) and bond-bending (β) interactions, is adopted to describe the elastic strain energy in a Si/Ge superlattice. For a Si/Ge superlattice grown pseudomorphically on a Si substrate, Si layers are free of strain whereas Ge layers are fully strained [8]. Ge layers experience thus a biaxial strain in the [110] and [1$\bar{1}$0] directions and a compressive strain in the [001] direction. It has been found [8] that the difference in interplanar spacings in a sublattice is quite small and can be neglected. The geometrical structures of Si/Ge superlattices are obtained by elastic strain energy minimization as done in [7, 8]. The results reveal that the Si–Si spacing is the same as that in bulk Si (1.358 Å) and the Si–Ge and Ge–Ge spacings are 1.408 Å and 1.468 Å, respectively.

The detailed description of the computational method for phonon spectra in Si/Ge superlattices has been presented in [7] and will not be repeated here. Calculated longitudinal phonon dispersion curves and corresponding displacement patterns at the zone centre ($\boldsymbol{q} = \mathbf{0}$) for $(Si)_n/(Ge)_m$ $(n + m = 8, 2 \leqslant n \leqslant 6)$ superlattices grown on Si(001) are shown in figures 1–5. The modes in the figures are numbered in the order of increasing frequency. The phonon symmetries at the reduced wavevector $\boldsymbol{q} = \mathbf{0}$ are also given in figures 1–5. The space groups to which $(Si)_n/(Ge)_m$ superlattices belong are listed in table 1. When the numbers of both Si and Ge layers are odd, the superlattices have no inversion centre. Moreover, the [110] and [1$\bar{1}$0] directions are equivalent, which

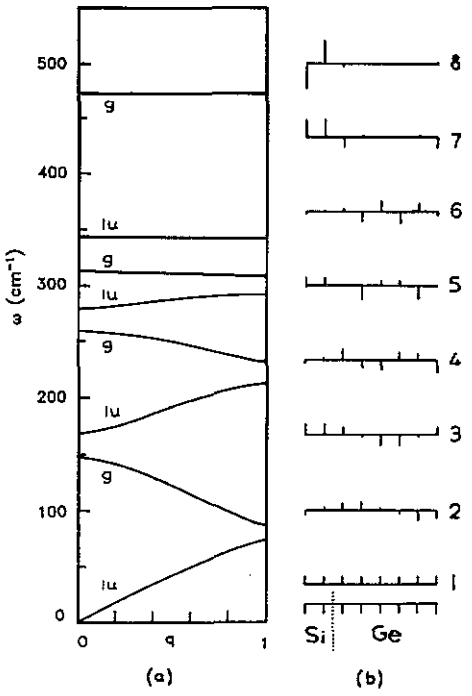

Figure 1. (*a*) Longitudinal phonon dispersion curves of a $(Si)_2/(Ge)_6$ superlattice on a Si(001) substrate; (*b*) displacement patterns at the zone centre. The label (only the subscript is used) gives the phonon symmetries at $q = 0$.

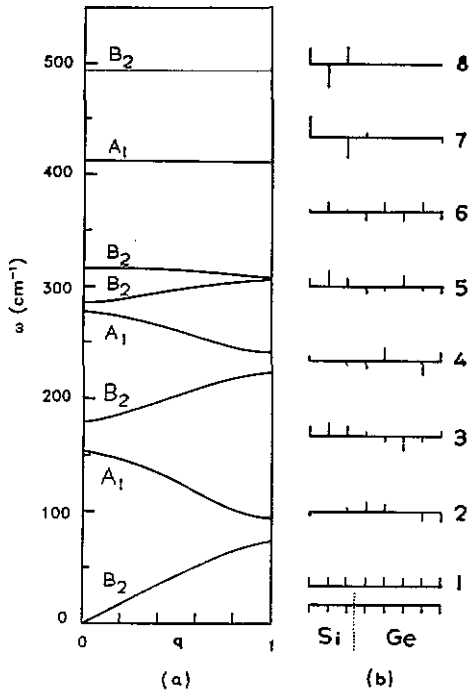

Figure 2. (*a*) Longitudinal phonon dispersion curves of a $(Si)_3/(Ge)_5$ superlattice on a Si(001) substrate; (*b*) displacement patterns at the zone centre. The label gives the phonon symmetries at $q = 0$.

leads to degeneracy of two transverse modes. For an even number of layers of Ge or Si, the superlattice has orthorhombic symmetry and the transverse modes of both polarizations split at $q = 0$ for $\omega \neq 0$.

For a $(Si)_2/(Ge)_6$ superlattice (figure 1), it is obvious that mode 8 is a Si-like confined LO mode. Mode 7 is a Si-like longitudinal acoustic (LA) mode, which can be clearly seen from the displacement pattern (figure 1(*b*)). The frequency is governed mainly by the thickness of Si layers and by the force consants of the Si–Ge bonds as well. Modes 4–6 are Ge-like quasi-confined LO modes. Modes 1–3 are folded LA modes resulting from the folding due to the reduction in Brillouin zone.

For a $(Si)_3/(Ge)_5$ superlattice (figure 2), modes 8 and 7 are the first- and second-order Si-like confined LO modes, respectively. Modes 4–6 are Ge-like confined LO modes. Note that there exists certain slight dispersion in modes 4–6 due to non-vanishing of vibrations in Si layers.

For a $(Si)_4/(Ge)_4$ superlattice (figure 3), there are two Si-like LO modes. Mode 6, with frequency higher than that of bulk Ge at the zone centre, is not a Si-like confined LO mode, although it is nearly dispersionless. This behaviour can be understood by the fact that this mode involves vibrations of Si layers and only interface Ge atoms, like mode 7 of a $(Si)_2/(Ge)_6$ superlattice (see figure 1). Modes 4 and 5 are Ge-like LO modes.

For a $(Si)_5/(Ge)_3$ superlattice (figure 4), three Si-like LO modes exist. Modes 8–6 correspond to the first-, second- and third-order Si confined LO modes, respectively. Clearly, mode 4 is a Ge-like LO mode.

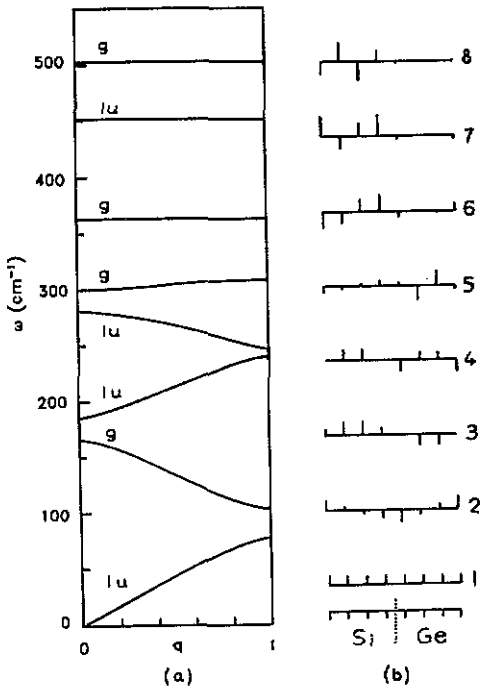

Figure 3. (*a*) Longitudinal phonon dispersion curves of a $(Si)_4/(Ge)_4$ superlattice on a Si(001) substrate; (*b*) displacement patterns at the zone centre. The label (only the subscript is used) gives the phonon symmetries at $q = 0$.

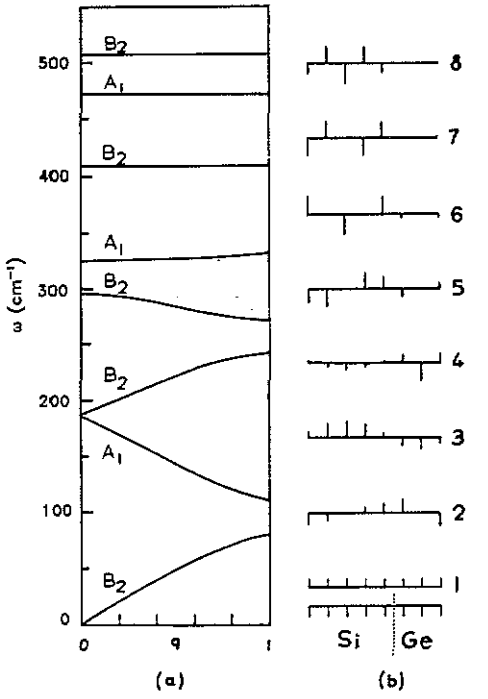

Figure 4. (*a*) Longitudinal phonon dispersion curves of a $(Si)_5/(Ge)_3$ superlattice on a Si(001) substrate; (*b*) displacement patterns at the zone centre. The label gives the phonon symmetries at $q = 0$.

Table 1. Space groups for $(Si)_n/(Ge)_m$ $(n + m = 8, 2 \leq n \leq 6)$ superlattices grown in the [001] direction and the phonon symmetries at $q = 0$ for longitudinal modes.

	n, m even	n, m odd
Space group	$D^5_{2h}(Pmma)$	$D^5_{2d}(P\bar{4}m2)$
Phonon symmetry	A_g, B_{1u}	A_1, B_2

For a $(Si)_6/(Ge)_2$ superlattice (figure 5), modes 8–6 are Si-like LO modes, corresponding to the first-, second- and third-order Si-like LO modes, respectively. Mode 5, like mode 6 in a $(Si)_4/(Ge)_4$ superlattice, is also nearly dispersionless. There is significant LA-like excitation of Si atoms in mode 4, a Ge-like LO confined mode, due to the small thickness of Ge layers.

The frequency shifts of optical modes in the Si/Ge superlattice (with respect to those in bulk Si and Ge) are affected by two contributions. The first is a shift due to strain and the second originates from the confinement of Si (Ge) optical modes in Si (Ge) layers. For Si/Ge superlattices grown on Si, there is no strain in Si layers. Hence the shift of a Si confined LO mode with respect to the bulk mode directly measures the confinement energy. In figure 6, phonon frequencies of the Si-like confined LO modes for $(Si)_n(Ge)_m$

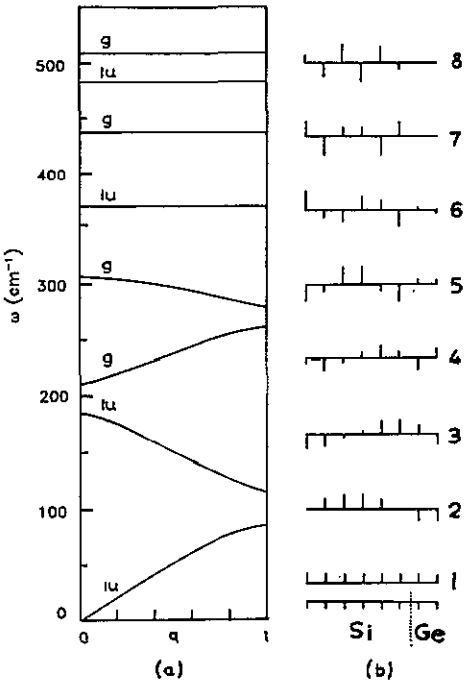

Figure 5. (*a*) Longitudinal phonon dispersion curves of a $(Si)_6/(Ge)_2$ superlattice on a Si(001) substrate; (*b*) displacement patterns at the zone centre. The label (only the subscript is used) gives the phonon symmetries at $q = 0$.

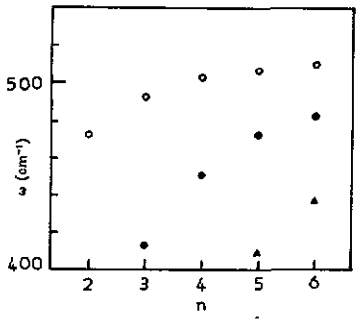

Figure 6. Phonon frequencies of Si-like confined LO modes versus the number n of Si layers: ○, first order; ●, second order; ▲, third order.

$(n + m = 8, 2 \leqslant n \leqslant 6)$ superlattices on Si(001) are shown. It is obvious that the confinement decreases with increasing thickness of the Si layers.

It can be seen from figures 1–5 that the number of Si-like confined LO modes increases with increasing number of Si layers. The confinement can be analysed similarly to the work of Sood *et al* [11]. The analysis is based on the idea that standing waves have to fit into a single slab. The mode frequency is then given by $\omega(q_{\text{eff}})$, where $\omega(q)$ is the bulk dispersion of the corresponding phonon modes. The effective reduced wavevector q_{eff} is defined (in units of $2\pi/a$, where a is the lattice constant of bulk material) as

$$q_{\text{eff}} = ja/2d_{\text{eff}} \tag{1}$$

where d_{eff} is the thickness of an effective slab and j is the order number of confined modes, numbered starting from the top. For Si/Ge superlattices grown on a Si(001) substrate, d_{eff} can be written as $d_{\text{eff}} = n_{\text{eff}}a/4$, where n_{eff} is the number of monolayers over which a mode actually extends. If n_{eff} is known, this consideration yields a correspondence between the superlattice confined modes and the bulk dispersion curves of the constituent materials. By comparing the frequencies of confined modes with bulk dispersion curves, it is found that, when $n_{\text{eff}} = n + 1$, the Si confined modes are described well by the bulk dispersion, where n is the number of monolayers of Si. Therefore, for Si confined LO modes, q_{eff} is given by

$$q_{\text{eff}} = j2/(n + 1). \tag{2}$$

Table 2. Comparison of frequencies of Si confined modes with those (in parentheses) obtained from bulk dispersion by equation (2).

	Frequency (cm^{-1}) for the following modes		
	$j = 1$	$j = 2$	$j = 3$
$(Si)_2/(Ge)_6$	473 (471)		
$(Si)_3/(Ge)_5$	493 (492)	412 (402)	
$(Si)_4/(Ge)_4$	502 (501)	451 (448)	
$(Si)_5/(Ge)_3$	507 (506)	472 (471)	409 (402)
$(Si)_6/(Ge)_2$	510 (509)	484 (484)	437 (436)

In table 2, the frequencies of Si confined modes are compared with those obtained from the bulk dispersion curves by means of equation (2). Obviously, the results are quite satisfactory, especially for small j. Thus, using the relation (2), the frequency of Si confined modes in Si/Ge superlattices can be obtained simply from bulk dispersion curves.

The number of Si confined modes can also be obtained by the fact that q_{eff} is less than the wavevector at Brillouin zone boundary along the [001] direction, i.e. $q_{\text{eff}} \leqslant 1$. This gives the total number of Si confined modes J:

$$J = \begin{cases} n/2 \\ (n+1)/2 \end{cases} \quad \text{for} \begin{cases} n \text{ even} \\ n \text{ odd.} \end{cases} \tag{3}$$

Compared with Si-like confined modes, Ge-like confined modes are not easily confined in Ge layers because of the coupling of the optical continuum of Ge with the acoustic continuum of Si. Since the Ge layers are fully strained, there are two factors affecting the frequencies of Ge-like confined LO modes: strain and confinement. The frequency shifts due to strain can be calculated from [12] and it has been found that this shift is 16 cm^{-1} towards higher energies. The phonon frequencies of Ge-like confined LO modes are also found to decrease with the confinement. This phenomenon can be understood in terms of the phonon quantum well picture [13], since the 'optical effective mass' is usually negative (negative dispersion of the optical phonon branches near the zone centre). The confinement of Ge-like modes are quite complex and detailed results will be discussed elsewhere [14].

3. Raman spectra of $(Si)_n/(Ge)_m$

The relative intensities of the Raman peaks are calculated using the bond polarizability model [1, 15]. For the Raman polarizability parameters, α_{xx} and α_{xy} of Si and Ge, it is assumed [15] that $\alpha^{Ge} = 2\alpha^{Si}$. For the Si–Ge bond the parameter α^{SiGe} is taken as the average of α^{Si} and α^{Ge}, i.e. $\alpha^{SiGe} = (\alpha^{Si} + \alpha^{Ge})/2$. In figures 7–11, Raman spectra at the zone centre are given for $(Si)_n/(Ge)_m$ ($n + m = 8$, $2 \leqslant n \leqslant 6$) superlattices grown on Si(001).

For a superlattice with the D_{2h}^5 space group, the longitudinal modes at the zone centre have symmetry of either A_g or B_{1u}. Only A_g modes are Raman active with the back-scattering configuration. There are three peaks in the Raman spectra of a $(Si)_2/$

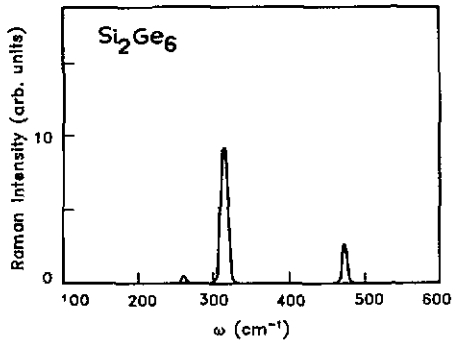

Figure 7. Raman spectra of a $(Si)_2/(Ge)_6$ superlattice grown on Si(001) at $q = 0$.

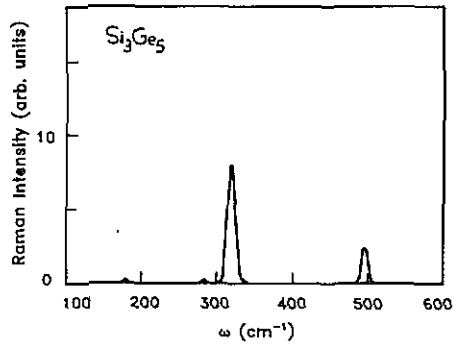

Figure 8. Raman spectra of a $(Si)_3/(Ge)_5$ superlattice grown on Si(001) at $q = 0$.

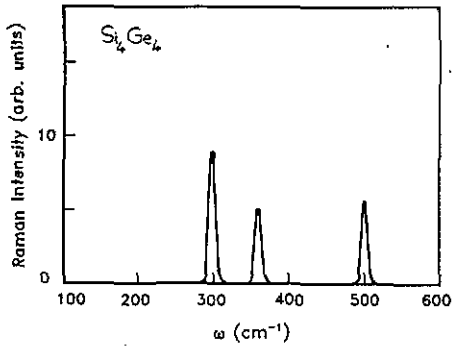

Figure 9. Raman spectra of a $(Si)_4/(Ge)_4$ superlattice grown on Si(001) at $q = 0$.

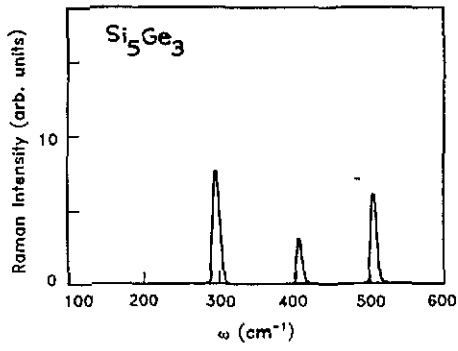

Figure 10. Raman spectra of a $(Si)_5/(Ge)_3$ superlattice grown on Si(001) at $q = 0$.

$(Ge)_6$ superlattice (figure 7). The peak at 473 cm^{-1} is from the topmost Si confined mode, the peak at 313 cm^{-1} from the first-order Ge-like confined LO mode, and the small peak at 260 cm^{-1} from the third-order Ge confined LO mode 4. Mode 2 is also Raman active, but its intensity is very small.

For a superlattice with D_{2d}^5 space group, the longitudinal modes at the zone centre belong to either A_1 or B_2 symmetry. In the $z(x, y)\bar{z}$ back-scattering configuration, only the modes with B_2 symmetry are Raman active and in the $z(x, x)\bar{z}$ configuration, only the modes with A_1 symmetry are Raman active, where $x = (100)$, $y = (010)$, $z = (001)$. For a $(Si)_3/(Ge)_5$ superlattice (figure 8), in the $z(x, y)\bar{z}$ configuration, there are four peaks (two strong and two weak) at 493, 317, 284 and 179 cm^{-1}, corresponding to Si confined mode 8, first-order Ge confined mode 6, second-order Ge confined mode 5, and folded LA mode 3, respectively. The Raman intensities of the peaks in the $z(x, x)\bar{z}$ configuration are too small to be detected.

The space group of a $(Si)_4/(Ge)_4$ superlattice is D_{2h}^5. Therefore only the A_g modes are Raman active. Three peaks appear in Raman spectra at 503, 364 and 299 cm^{-1}, corresponding to Si confined mode 8, Si confined mode 6 and Ge confined mode 5, respectively (see figure 9).

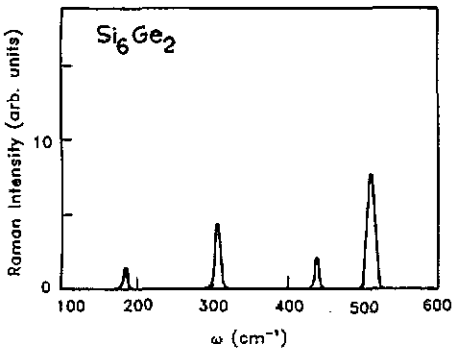

Figure 11. Raman spectra of a $(Si)_6/(Ge)_2$ superlattice grown on Si(001) at $q = 0$.

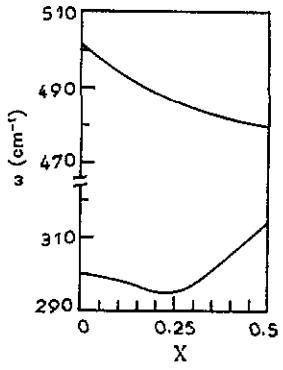

Figure 12. Phonon frequencies of first-order Si-like confined and Ge-like quasi-confined LO modes with respect to interface diffusion factor x for a $(Si)_4/(Ge)_4$ superlattice grown on Si(001).

Three peaks exist in the Raman spectra of a $(Si)_5/(Ge)_3$ superlattice (figure 10). The peaks at 507 and 409 cm^{-1} correspond to the Si confined modes. The peak at 296 cm^{-1} belongs to a Ge-like LO mode. It is interesting to note that the peak at 409 cm^{-1} is not an interface mode, but its Raman intensity is significant.

There are four peaks in the Raman spectra of a $(Si)_6/(Ge)_2$ superlattice (figure 11). The two peaks at 510 and 437 cm^{-1} correspond to Si confined modes 8 and 7, respectively. The peak in Raman spectra at 307 cm^{-1} results from Ge-like LO mode 4. A small peak at 211 cm^{-1} exists, corresponding to the folded LA mode 3.

In Raman experiments [1], in addition to the acoustical folded modes, a common feature also observed in all Raman spectra is the presence of three main peaks at around 300, 400 and 500 cm^{-1}, which are attributed to the Ge, Si–Ge and Si modes, respectively. In particular, the assignment of the peak around 400 cm^{-1} to the Si–Ge vibration is based on the comparison with the Si–Ge alloy. In our calculations there are modes at around 500 and 300 cm^{-1}, which are in good agreement with the Raman data. The so-called Si–Ge mode at around 400 cm^{-1}, however, does not appear in all the calculated Raman spectra in the longitudinal polarization. The disagreement between calculations and experiments might originate from the fact that the interfaces of epitaxial Si/Ge superlattices by MBE might not be perfect. A Si–Ge alloy might exist at the interface owing to the intermixing. It is quite possible that the peak at around 400 cm^{-1} represents the Si–Ge mode of the alloy presented at the interface [16, 17]. Therefore, it might be concluded from those experiments that the Raman spectrum at around 400 cm^{-1} gives information about the atomic ordering and roughness at the Si–Ge interface. Since the alloy at the interface has not been taken into account in all theoretical calculations [2, 3, 6, 7], this might explain the discrepancy between the calculated results and the experimental data. It is worth noting that, in all results obtained from calculations [2, 3, 6, 7], proper interface modes in transverse polarization at around 400 cm^{-1} always appear. The presence of alloy layers at the interfaces destroys the translational symmetry along the growth direction, leading to breakdown of the Raman selection rules. Therefore, the transverse interface modes might also give some contribution to the Raman peak at around 400 cm^{-1}.

4. Effect of interface diffusion on phonon frequency

The appearance of a peak at around 400 cm^{-1} in Raman experiments has attracted much attention [16, 17]. This peak has been attributed currently to interface roughness resulting in the formation of alloy layers at the Si–Ge interfaces [16, 17]. This section deals with the effect of interface diffusion on phonon frequencies, and not with the origin of the peak at around 400 cm^{-1} observed in experiments, which will be discussed elsewhere. A recent cluster calculation [18] by the extended Huckel method indicates that it is energetically favourable to exchange a Si atom for Ge at the Si–Ge interface. Hence the formation of alloy layers at the interface is a common feature in Si/Ge superlattices. As a consequence, phonon frequencies in Si/Ge superlattices may be shifted owing to interface diffusion, especially for the confined modes in thin Si/Ge superlattices since the optical modes confined in Si (Ge) are sensitive to the width and shape of the Si (Ge) layer. For the quantitative discussion of interface diffusion, the virtual-crystal approximation is used to analyse the effect of interface diffusion on phonon frequencies of confined modes by allowing the formation of a Si–Ge alloy at the interface. Let the Si and Ge atoms be replaced by effective $Si_{1-x}Ge_x$ and Si_xGe_{1-x} atoms at the interface, respectively, where x is a factor determining the interface diffusion. The virtual-crystal potential of the alloy $Si_{1-x}Ge_x$ is given by

$$V(r) = (1 - x)V_{Si}(r) + xV_{Ge}(r) \tag{4}$$

where V_{Si} and V_{Ge} are the potentials of bulk Si and Bulk Ge, respectively. The mass of an effective $Si_{1-x}Ge_x$ atom is written as

$$M(Si_{1-x}Ge_x) = (1 - x)M(Si) + xM(Ge) \tag{5}$$

where $M(Si)$ is the atomic mass of a Si atom.

In figure 12 the variation in first-order Si- and Ge-like confined LO modes for a $(Si)_4/(Ge)_4$ superlattice grown on a Si(001) substrate with respect to the interface diffusion factor x is given. It is found that the first-order Si confined LO mode decreases with increasing x. This is more significant for higher-order Si confined LO modes; whereas for Ge-like confined modes it is much more complicated. It is seen from figure 12 that for $x < 0.25$ the frequency of the Ge confined mode decreases with increasing x and increases with increasing x for $x > 0.25$ because of the coupling of the optical continuum of Ge with the acoustic continuum of Si. For folded LA modes in Si/Ge superlattices, the phonon frequency shift due to the interface diffusion is relatively small, especially for the low-frequency modes, since the acoustic phonons are essentially sensitive to the periodicity of the superlattice and not to the interface roughness [19]. Therefore, from the above analysis, the phonon frequencies of Si confined modes can be viewed to some extent as a measurement of interface diffusion.

5. Conclusions

In the present work, phonon spectra of strained $(Si)_n/(Ge)_m$ $(n + m = 8, 2 \leqslant n \leqslant 6)$ superlattices grown pseudomorphically on a Si(001) substrate are studied using a generalized two-parameter Keating model. Raman spectra are also calculated by a bond polarizability model. Our calculations are compared with experimental data. It is pointed out that the Si-like confined modes can be well described by the bulk dispersion curves with the effective confinement length of Si layers being $(n + 1)a/4$. In the case of Ge

confined modes, it is difficult to define an effective confinement length because of the complexity caused by the overlapping of the optical continuum of Ge with the acoustic continuum of Si. No interface modes exist in the longitudinal polarization for Si/Ge superlattices with abrupt interfaces. The appearance of a peak at around 400 cm^{-1} in experiments is due to the contribution of alloy layers formed at the interfaces as a result of interface diffusion. Within the virtual-crystal approximation, phonon frequency shifts due to interface diffusion are investigated. The phonon frequencies of Si confined modes are shifted downwards with interface diffusion. The folded LA modes in Si/Ge superlattices are only slightly affected.

References

[1] Jusserand B and Cardona M 1989 *Light Scattering in Solid V* ed M Cardona and G Guntherodt (Berlin: Springer) p 49
[2] Molinari E and Fasolino A 1989 *Appl. Phys. Lett.* **54** 1220
Fasolino A and Molinari E 1987 *J. Physique Coll.* C5 569
[3] Alonso M I, Cardona M and Kanellis G 1989 *Solid State Commun.* **69** 479
[4] Kanellis G 1987 *Phys. Rev.* B **35** 746
[5] Keating P N 1966 *Phys. Rev.* **145** 637
[6] Ghanbari R A and Fasol G 1989 *Solid State Commun.* **70** 1025
[7] Zi J, Zhang K and Xie X 1990 *Phys. Rev.* B **41** 12 862
Zi J, Zhang K and Xie X 1990 *J. Phys.: Condens. Matter* **2** 2473
[8] Zi J, Zhang K and Xie X 1990 *Appl. Phys. Lett.* **57** 157
[9] Colvard C, Gant T A, Klein M V, Merlin R, Fischer R, Morkoc H and Gossard A C 1985 *Phys. Rev.* B **31** 2080
[10] Fasolino A, Molinari E and Maan J C 1989 *Phys. Rev.* B **39** 3923
[11] Sood A K, Menendez J, Cardona M and Ploog K 1985 *Phys. Rev. Lett.* **54** 2111
[12] Cerdeira F, Buchenaer F, Pollak F H and Cardona M 1972 *Phys. Rev.* B **5** 580
[13] Jusserand B, Paquet D and Regreny A 1985 *Superlatt. Microstruct.* **1** 61
[14] Jian Zi, Kaiming Zhang and Xide Xie 1991 unpublished
[15] Go S, Bilz H and Cardona M 1975 *Phys. Rev. Lett.* **34** 580
[16] Alonso M I, Cerdeira F, Niles D and Cardona M 1989 *J. Appl. Phys.* **57** 2645
[17] Menendez J, Pinczuk A, Bevk J and Mannaerts J P 1988 *J. Vac. Sci. Technol.* B **6** 1306
[18] Zhang Y 1990 unpublished
[19] Jusserand B, Alexandre F, Paquet D and Roux G L 1985 *Appl. Phys. Lett.* **47** 301